Effect of Kinematic Soil-Structure Interaction on the Foundation Motion of Integral Abutment Bridges

Kianosh Ashkani Zadeh [1], Carlos E. Ventura [2], William D. L. Finn [3]

[1] Ph.D. Candidate, Department of Civil Engineering, University of British Columbia, Vancouver, B.C. Canada.
[2] Professor, Dept. of Civil Engineering, University of British Columbia, Vancouver, B.C. Canada.
[3] Professor Emeritus, Dept. of Civil Engineering, University of British Columbia, Vancouver, B.C. Canada.

ABSTRACT

Due to Soil-Structure Interaction (SSI) effects, a bridge foundation experiences an excitation that might be significantly different from that at the free-field. This phenomenon is investigated for an integral abutment bridge. A continuum representation of soil and structure are constructed and used in response time history analyses. To isolate the kinematic SSI effect, foundation and bridge structure are simulated as mass-less. A set of ten selected ground motions is applied to soil only and soil+structure models. The free-field response is calculated from dynamic analysis of the soil model when excitation is applied to the bedrock. A similar approach is used for soil+structure model where foundation motion is extracted.

A finite element model developed based on the Meloland Road Overpass (MRO) is used as the case study in this research. Response Time History analyses using ten unscaled ground motions are performed. Spectral responses of free-field and foundation motions are chosen to objectively compare the variation of motions of the free-field and SSI models. In the case studied here, investigation of calculated spectra showed that in the short-period regime, the effect of kinematic SSI can significantly change the spectral acceleration observed at the foundation when compared to the free-field motion. Simulation results show that an amplification of the free-field motion takes place in a long period range that covers the first few natural periods of the system.

The applicability of the tau-average method is then investigated. It is shown that foundation motion estimation based on the tau-averaging method is unable to predict the amplification regime observed in the simulations.

Keywords: Integral Abutment Bridges (IAB), Response Time History (RTH) Analysis, Soil-Structure Interaction (SSI), Kinematic effect, Tau-averaging Method.

INTRODUCTION

Soil-Structure Interaction (SSI) has a significant impact on the response of bridge structures subjected to strong earthquakes. Despite the body of research on this topic, there are still areas that are not well understood. Furthermore, design codes do not cover many aspects of SSI effect in their provisions [1], [2], and [3]. SSI influences the system response in two ways: a) effect of foundation on altering ground motion (kinematic effect) and b) the effect of soil on the response of the structure (inertial effect).

In this study, a finite element (FE) model based on the Meloland Road Overpass (MRO) in California is used to consider the kinematic effect of SSI for Integral Abutment Bridges (IAB). This overpass is located near the Imperial Fault Zone in southern California and has experienced a number of earthquakes including the Imperial Valley earthquake in 1979. The bridge consists of a two-span integral abutment with a single row pile foundation. The main goal of this research is to provide an understanding on the variation of motion from free-field to foundation base of an integral abutment bridge. To achieve this goal, the following objectives are considered: a) investigate amplification or reduction of the foundation motions; and b) investigate the applicability of the Tau-average method proposed by Clough and Penzien [4] for estimating foundation motion in integral abutment bridges. Continuum models of soil deposit and Soil+Bridge are constructed and simulated using the Abaqus FEA software [5]. Response time history analysis is performed by applying ten unscaled strong motions chosen from the PEER NGA West-2 Ground Motion Database [6]. The concept of transmissibility function is employed to study amplification or reduction of foundation motion from the free-field motion. This paper includes four sections. In the section two, the difference between free field and foundation motions are investigated using finite element method. In this section a brief description of the model and FE analyses are presented, and transmissibility concept is applied to determine amplification and de-

amplification of the motion. Third section of the paper is on the Tau-averaging method where the capability of the method to accurately estimate the foundations' motion is examined. Finally concluding remarks are presented in the last section.

2. COMPARISON OF FREE FIELD AND BRIDGE FOUNDATION MOTIONS

A detailed 3D continuum model is developed for this study. Time history analysis was performed using the Abaqus FEA [5]. A continuum representation of soil, foundation, and the bridge was constructed and analyzed. To investigate the difference between bridge foundation motion and the free-field motion, two models are developed:

a) Soil Model

b) Soil + Bridge Model (SSI model)

2.1 Models Descriptions and FE Approach

The soil model is developed as an elastic continuum medium with soil material parameters summarized in Table 1. The model includes a simplified representation of the soil surrounding bridge underpass as shown in Figure 1(d). Infinite Boundary Elements (IBEs) are used as Absorbing Boundary Conditions (ABCs) in the model's boundary walls to simulate unbounded domain. IBEs ensure that energy is dissipated at the model edges rather than reflecting into the system. It serves to represent the far-field regions and provide "quiet" boundaries to the FE model in dynamic analyses [5]. The soil+structure model includes a simplified representation of a 63.4m long two-span concrete box girder bridge with a single pier column and the integral abutments which each supported by a single row pile foundation and surrounding soil. The key structural components of the bridge including abutment, pier column, deck slab, foundations and piles, and wing walls are considered in the model. The model also includes an extended representation of the soil embankment behind the abutment backwalls due to its significance in the system response (see Figures 1(a), 1(b), and 1(c)).
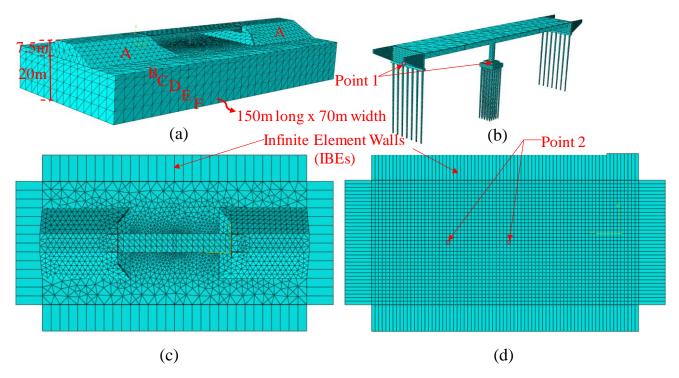

Figure 1. a) Discretized layout plan and 3D view of the soil and Soil+Bridge structure (SSI) model with showing finite element mesh, b) massless structure modeled in the SSI model and measurement points, c) discretized layout plan and infinite element boundary walls of the SSI model, and d) discretized layout plan and infinite element boundary walls of the soil free-field model and measurement points

Table 1. Material properties of the soil layers.

Soil Layer	Thick. (m)	Density (ρ) Kg/m³	Bulk Modulus (B) (MPa)	Shear Modulus (G) (MPa)	Modulus of Elasticity (E) (MPa)	Poison Ratio (v)	Shear Wave Velocity (Vs)
Gravel Clay (A)	7.43	1600	90	19	53.3	0.40	109.0
Medium Clay (B)	2.17	1500	300	60	169	0.41	200.0
Medium Sand1 (C)	3.36	1900	200	75	200	0.33	198.7
Stiff Clay1(D)	4.57	1800	750	150	422	0.41	288.7
Medium Sand2 (E)	4.57	1900	200	75	200	0.33	198.7
Stiff Clay2 (F)	5.33	1800	750	150	422	0.41	288.7

Density, bulk and shear modulus of the soil layers are adopted from the previous studies conducted by Kwon and Elnashai [7]. Modulus of elasticity, shear wave velocity and poison ratio of the soil layers are calculated using the following relationships:

$$v = \frac{3B - 2G}{2(3B + G)}, \; v_s = \sqrt{\frac{G_{max}}{\rho}} \; and \; E = 2G_{max}(1 + v) \tag{1}$$

where, G_{max} is the maximum shear modulus.

Rayleigh damping coefficients ($\alpha \; and \; \beta \; [\mathbf{C} = \alpha\mathbf{M} + \beta\mathbf{K}]$) used in both bridge and soil models.

2.2 Ground Motions

A set of ten un-scaled ground motions from the NGA-West2 ground motion database of the Pacific Earthquake Engineering Research Center (PEER) [6] is chosen to perform response history analysis in soil and SSI models, respectively. In this study, a significant duration corresponds to a maximum 95% arias intensity of the motions are used as input motion. Spectra of the selected input motions for comparison are shown in Figure 2. The characteristics of the selected input motions are shown in Table 2.

Table 2. The selected ground motions and their characteristics.

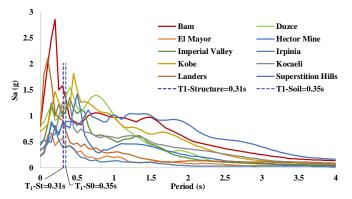| Earthquake Name	PEER RSN No	Year	Station Name	M	Predominant Period(s) / PGA (g)	Mechanism
Imperial Valley-06	184	1979	El Centro Differential Array	6.53	0.40/0.48	strike slip
Superstition Hills-02	723	1987	Parachute Test Site	6.54	0.64/0.43	strike slip
Kobe-Japan	1119	1995	Takarazuka	6.9	0.46/0.70	strike slip
Hector Mine	1787	1999	Hector	7.13	0.50/0.33	strike slip
Duzce-Turkey	1602	1999	Bolu	7.14	0.4/0.81	strike slip
Kocaeli-Turkey	1158	1999	Duzce	7.51	0.38/0.36	strike slip
Landers	879	1992	Lucerne	7.28	0.08/0.79	strike slip
Bam-Iran	4040	2003	Bam	6.6	0.20/0.81	strike slip
El Mayor-Cucapah-Mexico	5836	2010	El Centro - Meloland Geot. Array	7.2	0.18/0.23	strike slip
Irpinia Italy-01	288	1980	Brienza	6.9	0.14/0.22	Normal

Figure 2. Response spectra of the selected input motion with 5% damping and periods of interest.

2.3 Analysis

Eigenvalue analyses are performed first to calculate the natural periods and mode shapes of the system. The eigenvalue analysis is also employed to determine the Rayleigh damping coefficients of the soil model to be used in the time history analysis. Periods and mode shape description of the first six modes of the Soil and SSI models are presented in Table 3.

Table 3. Period and mode shape of the soil and Soil+Bridge models.

Mode	Soil Model		SSI model	
	Period (Frequency) T_i (s)[f_i (Hz)]	Mode Description	Period (Frequency) T_i (s)[f_i (Hz)]	Mode Description
1	0.35[2.89]	Longitudinal Mode	0.31[3.21]	Vertical anti-symmetric mode
2	0.34 [2.92]	Transverse Mode	0.28[3.52]	Transverse mode
3	0.33 [2.99]	1st. Torsional mode	0.23[4.34]	Vertical symmetric mode
4	0.33 [3.05]	2nd. Longitudinal Mode	0.15[6.74]	1st. Torsional mode
5	0.32 [3.13]	2nd. Transverse Mode	0.10[9.72]	2nd. Torsional mode
6	0.31 [3.23]	2nd. Torsional mode	0.09[11.36]	2nd. Vertical anti-symmetric mode

Due to various dissipative mechanisms involved, damping of a soil-structure system becomes a complex topic. Various researchers and code provisions suggest a range of damping ratios for the entire soil-structure system. In 1969, The U.S. Nuclear Regulatory Commission defines an upper limit of 15% to total soil-structure interaction damping [8]. Caltrans's seismic design criteria suggests a 10% total damping ration for bridges that are heavily influenced by energy dissipation at the abutments [9]. Feng and Lee [10] suggest a damping ratio between 3 to 12% for the entire bridge system. These suggested damping values are for the entire bridge system that includes contributions from both soil and the structure. In this study, Rayleigh damping with two separate damping ratios are incorporated for the soil and the concrete components. As suggested by Kwon and Elnashai [7] a damping ratio of 4% is applied to structural components on modes 1 and 10 (see Figures 3(b) and 3(c)). The modal frequencies are adopted from the ambient vibration tests as reported by Ventura et al. [11]. A damping ratio of 12.5% is applied to soil layers including the abutment embankments on modes 1 and 12 (see Figure 3(a)). As discussed earlier, in addition to Rayleigh damping, the soil model includes non-reflecting boundary condition that incorporates the effect of radiation damping.
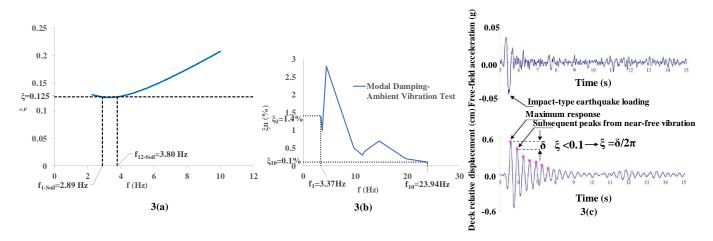

Figure 3. Identification of damping properties of the MRO: a) Damping ratio vs. frequency for the soil layers, b) bridge damping ratio vs. frequencies obtained from the Ambient Vibration Test [11], and c) decaying and damping ratio of the superstructure identified by Kwon and Elnashai [7].

Using 10 un-scaled ground motions (listed in Table 2), Response Time History (RTH) analyses are then performed to investigate the effect of SSI on foundation motion when compared to free-field motion. To extract the free-field motion, RTH analysis is performed on the soil model applying input excitation at the rock base (bottom of the supporting deposit soil). In all models, ground motion is applied along the deck direction. Direct output of the finite element simulation in terms of time history accelerograms does not provide insight into the behavior of the system as comparison of the peak accelerations does not offer an objective measure of the response. Spectral acceleration on the other hand offers a more objective assessment of the system behavior and is consistent with code provisions.

2.4 Effect of Kinematic Soil-Structure Interaction in Foundation Motion: Amplification or Reduction?

To study the variation of the bridge foundation motion from the free-field motion, the concept of transmissibility function is employed here. Transmissibility Function (TF) is defined by the ratio between the Fourier transform of the bridge foundation

acceleration ($\ddot{u}_{bf}$) to that of the free-field acceleration ($\ddot{u}_{ff}$), as given in Eq. 2. This function can be used to determine the spectral amplifications and reduction as a function of frequency.

$$TF(\omega) = \frac{FT(\ddot{u}_{bf})}{FT(\ddot{u}_{ff})} = A(\omega)e^{i\theta(\omega)} \tag{2}$$

where, FT is the Fourier Transform function, $A(\omega) = |TF(\omega)|$ is the amplitude of the transmissibility function, and $\theta(\omega)$ is the phase angle. The numerical evaluation of Eq. 2 is performed using the Fast Fourier Transform (FFT) algorithm. Figure 4 shows the transmissibility amplitude (*A*) as a function of frequency. This is obtained using the response of points 1 and 2 as shown in Figure 1.
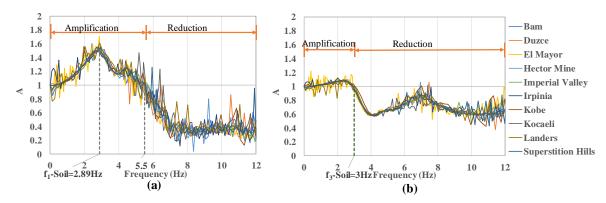

Figure 4. Transmissibility factors calculated from RTH analyses for a) abutment footing foundation and b) pier foundation.

As shown in the above figure, the pier foundation shows an initial slight amplification up to 3Hz which corresponds to soil's third mode frequency ($f_{3\text{-Soil}} \approx 3$Hz). Past this point, reduction is observed. The abutment footing foundation motion shows an amplification in the frequency range below 5.5Hz with the peak occurring at soil's natural frequency of 2.89Hz ($f_{1\text{-Soil}}$). A de-amplification is also observed in the abutment motion past 5.5Hz range. It is worth noting that the natural period of the bridge system resides within the amplification regime. As a result, analysis based on the free-field excitation would underestimate the bridge response.

3. APPLICABILITY OF TAU-AVAERAGING METHOD TO ESTIMATE FOUNDATION MOTION

3.1 Tau-averaging Method

Slab averaging caused by interaction of the rigid foundation and the earthquake wave leads to a reduction in the magnitude of motion experienced by the foundation. This effect is more significant when the foundation dimension is large relative to excitation wave length. When foundation dimensions along the direction of the earthquake wave propagation are larger than wavelength, an averaging effect would take place which will result in a reduction in the foundation motion's magnitude when compared to free field motion. Reduction in the magnitude of the motion at the foundation increases when the ratio of dimension of the foundation to the wave length of the motion increases [4].

Newmark et al. [12] introduced a numerical averaging scheme to estimate the foundation motion from the free field. Clough and Penzien [4] later proposed a method based on averaging of harmonic waves, known as tau-averaging scheme. This approach assumes a mass-less rigid slab foundation and calculates the averaging of the incoming wave due to its kinematic interaction with the foundation. In the tau-average method, the Fourier Transform of the foundation motion is estimated by applying a reduction multiplier, τ, to the Fourier Transform of the free-field motion as shown in Eq. 3.

$$FT\left(\ddot{u}_{bf}^{est}\right) = \tau(\omega)\ FT\left(\ddot{u}_{ff}\right) \tag{3}$$

The foundation acceleration in time domain ($\ddot{u}_{bf}^{est}$) is then calculated using the inverse Fourier Transformation as shown in Eq. 4.

$$\ddot{u}_{bf}^{est} = IFT\left(\tau(\omega)\ FT\left(\ddot{u}_{ff}\right)\right) \tag{4}$$

The factor τ is a function of the frequency (ω), the foundation dimension along the wave direction (D) and apparent wave velocity (V_a) as shown in Eq. 5.

$$\tau = \frac{1}{\alpha}\sqrt{2(1-\cos\alpha)} \quad \text{where,} \quad \alpha = \frac{\omega D}{V_a} = \frac{2\pi D}{\lambda(\omega)} \tag{5}$$

When base dimension of the foundation (D) is large compared with the wavelength of the ground motion $(\lambda = 2\pi\frac{V_a}{\omega})$, the tau-effect is significant, and the resulting averaged magnitude of foundation motion will be smaller than the free-field ground motion. Abutment foundation dimension along the encountering seismic wave is about 0.9m whereas the pier pile cap foundation dimension is about 4.6m. Therefore, as shown in Figure 5(a) the tau factor is almost equal to 1.0 for abutment footing due to its relatively small foundation dimension comparing to wave length of the ground motions. As a result, the abutment foundation has little kinematic effect on the ground motions and the tau-averaging method predicts a foundation motion that is almost identical to the free-field motion. This is confirmed by Figure and 5(b) which shows that the free field motions are unaffected by application of the τ factor.
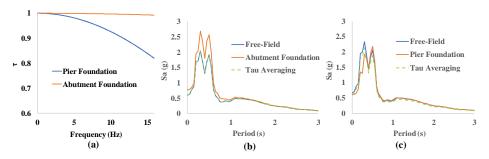

Figure 5. a) calculated Tau parameter for abutment and pier foundations, Comparison of Hector Mine spectrum with 5% damping of a foundation motion with the free-field and estimated foundation motion using tau-averaging method b) Abutment footing foundation, and c) pier pilecap foundation.

The tau-averaging method introduces a simplified approach to incorporate base slab averaging due to kinematic constraint caused by the stiff surface foundation. This method was originally designed for mat slab foundations and does not capture other kinematic SSI aspects such as embedment and wave scattering effects.

It is considered that the stiffness of massless foundations results in base slab averaging and preventing them from matching free-field deformations. However, as it was shown earlier, the tau-averaging method did not accurately estimate the foundation motions for the abutment and pier foundations in this case study. Tau parameter is always less or equal to one as it is only relying on base slab averaging effect, therefore it cannot predict amplification of the foundation motion due to the embedment and wave scattering effects. The amplification observed for abutment foundation is believed to be mainly due to embedment effect due to increase in the height of the soil at the abutment footing foundation compared to the ground grade level, at which the free field motion is observed. Chang et al. have investigated the effect of depth on intensity of the motion in soil. According to this work, both peak acceleration and response spectra of ground notions significantly varied with depth [13]. Elevation of the Abutment footing and Pier pilecap foundation are shown and compared with the ground level in Figure 6. The slight amplification of the Pier foundation can be due to other aspects of kinematic SSI such as vertically propagated shear waves and the wave scattering effect of footing and pilecap foundations. As discussed by Gicev et al. [14], wave propagation along the base of the structure must be considered for structures with multiple supports. This effect can lead to rocking and foundation translation.
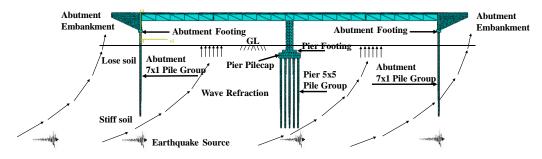

Figure 6. One dimensional shear beam site amplification. Abutment embankment is not shown for clarity.

To assess the performance of the Tau method in averaging the foundation motion, the spectra of the estimated motions are compared with the spectra of foundation motion calculated from FE analysis. SeismoSignal software [15] was employed to calculate the spectra of free-field motion, estimated foundation motion as well as foundation motion extracted from FE simulation. Figure 7 and Figure 8 show a comparison of the spectral acceleration for the Abutment and Pier foundations for the Imperial Valley, Landers, and El Mayor ground motions, respectively.
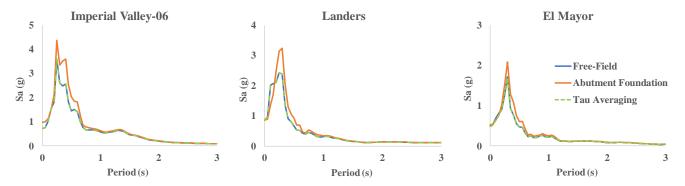

Figure 7. Spectra of the Abutment footing foundation, free-field, and estimated foundation based on the Tau-averaging method with 5% damping.
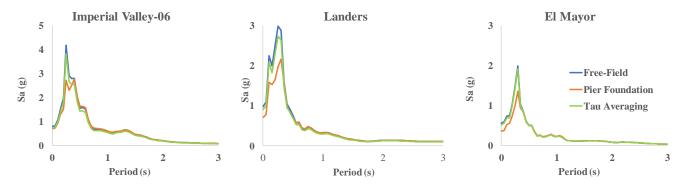

Figure 8. Spectra of the Pier pilecap foundation, free-field, and estimated foundation based on the Tau-averaging method with 5% damping.

A more comprehensive comparison of spectral accelerations can be found in [16]. To obtain a measure of accuracy of the Tau-averaging method in estimating the spectral acceleration of the foundation motion, an error estimator is defined as per Eq. 6:

$$Error\% = \frac{1}{\sqrt{N}} \sqrt{\frac{\sum (Sa_{Tau} - Sa_{Found})^2}{Sa_{Found}^2}} \times 100 \tag{6}$$

in the above equation, Error (%) is defined as an average of ratio of the pairwise Euclidian distance between the spectral accelerations and foundation spectral acceleration. The predicted error for each analysis is listed in Table 4.

Table 4. Error in estimated motion using Tau-averaging method compare to foundation motion.

Event/Foundation	Error of the Estimated Motions by Tau-averaging Method (%)	
	Abutment Footing	**Pier Pilecap**
Imperial Valley-06	12.2	11.6
Superstition Hills-02	10.8	11.1
Kobe-Japan	12.4	12.5
Hector Mine	12.8	12.4
Duzce-Turkey	12.3	12.3
Kocaeli-Turkey	13.2	11.0
Landers	13.9	13.4
Bam-Iran	10.5	14.4
El Mayor-Cucapah-Mexico	11.3	13.5
Irpinia-Italy-01	14.0	12.8

As it can be seen from the Table 4, the estimated foundation motion using the Tau-averaging method shows a difference of up to14.5% difference from foundation motion calculate from FE analysis for the abutment and pier foundations.

4. CONCLUDING REMARKS

In this research, numerical simulation was used to investigate the kinematic aspect of soil-structure interaction effect on an integral abutment bridge. The comparison of the bridge's abutment footing and pier pile cap foundation motions with the free-field motion showed zones with amplification of the excitation (in the lower frequency regime) and zones that exhibit reduction (in the higher frequency regime). The tau-averaging method was applied to estimate bridge foundation motion and it was shown that this method is not capable of capturing the amplification regime in the short frequency ranges. It is important to note that the natural frequency of the bridge system resides within the amplification regime. Therefore, use of the spectra from the free-field in design may lead to an underestimated design. In addition to the slab averaging mechanism that leads to reduction in excitation magnitude, there are other kinematic SSI effects (e.g. embedment effect, wave scattering and vertically propagated shear waves) that can lead to amplification of the foundation motion compared to the free-field. Further studies are ongoing to assess the generality of the observations.

REFERENCES

[1] Mitchell, D., Bruneau, M., Williams, M., Anderson, D., Saatcioglu, M., and Sexmith, R. (1995). "Performance of bridges in the 1994 Northridge Earthquake." *Canadian Journal of Civil Engineering*; 22, 415-427.

[2] Mylonakis, G., Nikolaou, A., and Gazetas, G. (1997) "Soil-pile-bridge seismic interaction: Kinematic and inertial effects." *Earthquake Engineering and Structural Dynamics*; 26, 337-359.

[3] Barbosa, A., Mason, B., and Romeny, K. (2014). "SSI-Bridge: Soil-bridge interaction during long-duration Earthquake motions." *Corvallis: Pacific Northwest Transportation Consortium (Pac Trans)*.

[4] Clough, R.W., Penzien, J. (1995) "Dynamics of Structures", 3rd. Edition. *Computers & Structures: Berkeley*, Inc.

[5] SIMULIA (2018). Accessed, from https://www.3ds.com/products-services/simulia/

[6] Pacific Earthquake Engineering Research Center (PEER). PEER NGA online ground motion database, (2018). Retrieved from PEER Ground Motion Database: http://ngawest2.berkeley.edu/

[7] Kwon, O. S. and Elnashai, A. S. (2008), "Seismic analysis of Meloland Road Overcrossing using multiplatform simulation software including SSI", *Journal of Structural Engineering* 134(4), 651–660.

[8] Stevenson, J. D. (1980). "Structural damping values as function of dynamic response stress and deformation levels." *Nuclear Engineering and Design* 60 211-237.

[9] Caltrans (2013). "Seismic Design Criteria, version 1.7." *California Department of Transportation*.

[10] Feng, M. Q., Lee, S. C. (2009). Determining the effective system damping of highway bridges. *Department of Civil & Environmental Engineering, University of California, Irvine*.

[11] Ventura, C.E., Carvajal, J. C., Liam, Finn L., and Traber, J. (2011). "Ambient Vibration Testing of the Meloland Road Overpass". *4th. International Operational Modal Analysis Conference (IOMAC 2011)*.

[12] Newmark, M., Hall, W. J. and Morgan, J. R. (1977). "Comparison of building response and free field motion in Earthquake." *Proceedings of 6th World Conference on Earthquake Engineering, New Delhi, India*.

[13] Chang, C. Y., Tseng, W. S., Tang, Y. K., (1989). Power, M. S., "Variations of Earthquake ground motion with depth and its effect on soil-structure interaction. " *Second DOE Natural Hazards Mitigation Conference*.

[14] Gicev, V., Trifunac, M. D., Orbović, N. (2016). Two-dimensional translation, rocking, and waves in a building during soil-structure interaction excited by a plane Earthquake SV-wavepulse

[15] SeismoSignal (2018). Earthquake Engineering Software Solution, Italy. http://www.seismosoft.com/.

[16] Ashkani Zadeh, K. (2019). "Effect of soil-structure interaction on performance-based design of integral abutment bridges." *PhD Thesis (in preparation). The University of British Columbia, Vancouver, Canada*.